

JOURNAL OF SCIENTIFIC INSTRUMENTS

VOL. XVI

AUGUST 1939

No. 8

AMPLIFICATION BY SECONDARY ELECTRON EMISSION.

By W. H. RANN, Radium Beam Therapy Research, Medical Research Council, London

[MS. received 13th January 1939]

ABSTRACT. The experimental data relating to the phenomenon of secondary electron emission from simple and complex surfaces is collected and tabulated. Simple electron multipliers with single stages of multiplication are examined and typical characteristics are shown. A brief description is given of the now obsolete dynamic type. Full details and operating characteristics of multi-stage electron multipliers using combined electrostatic and magnetic focusing are then given. The final section deals with electron multipliers using only electrostatic focusing. This last group is divided into two classes consisting of multipliers with solid targets and those with grid mesh targets.

INTRODUCTION

THE phenomenon of secondary electron emission from various surfaces when bombarded with cathode rays has been known for the past thirty years. When an electron strikes a surface it may either be reflected, or be absorbed with or without the liberation of other electrons. The reflexion of electrons generally occurs when their energy is less than 10 eV. The emission of secondary electrons, however, becomes more marked as the energy of the primary electrons increases. The secondary electrons, so-called from their mode of origin, have energies of all values up to that of the primary electron, but the bulk of them have energies of less than 20 eV.

It has been recognized for many years⁽¹⁻⁵⁾ that if this phenomenon could be applied to the amplification of small electron currents a very simple and effective substitute for the conventional thermionic valve amplifier would be obtained.

The secondary electron emission from simple surfaces has been examined both experimentally^(6-22, 24-25) and theoretically⁽²³⁾ by various workers. Table I gives the collected experimental results together with other relevant data, including the work function of the surface and the energy of the primary electron.

The secondary electron emission from complex surfaces is much more complicated. The experimental results are collected in Table II, and it can be seen that the values obtained are often contradictory, due no doubt to indefiniteness of the experimental conditions.

Treloar⁽²²⁾ and Sixtus⁽¹²⁾ have shown that there is a relation between the work function of a surface and its coefficient of secondary electron emission inasmuch as a reduction of the work function is accompanied by an increase in the coefficient of secondary electron emission.

From Table II it may be seen that the compound surfaces of the type Ag-CsO-Cs give the most copious yield of secondary electrons. Fig. 2 shows the relation between the energy of the bombarding electron (primary electron) and the number of secondary electrons liberated from a surface of this type. For other surfaces, curves of approximately the same general shape are obtained, but the maxima may be displaced to regions of lower or higher energies of the primary electrons.

TABLE I. *Collected experimental results concerning secondary electron emission*

Metal	Coefficient of secondary emission δ max.	v. primary in volts	Work function in volts	Atomic Weight	Reference
Lithium	0.56	100	2.28	6.94	21
	0.48	75	—	—	21
Beryllium	0.90	100-200	3.16	9.02	25
	0.53	200	—	—	21
Magnesium	0.95	300	2.42	24.32	21
	1.10	220	—	—	6
Aluminium	0.97	300	2.26	26.97	21
Iron	1.0	300	—	55.84	7
	1.3	348	—	—	9
Nickel	1.2	400	5.03	58.7	20
	1.3	600	—	—	20
	1.3	455	—	—	9
	2.5	400	—	—	25
	2.1	440	—	—	25
	1.3	450	—	—	14
	1.2-1.3	500	—	—	21
Copper	1.12	250	—	63.57	13
	1.32	240	—	—	8
	1.04	250	—	—	6
Molybdenum	1.25	375	4.15	96	21
	1.19	600	—	—	11
	1.00	2000	—	—	11
	1.30	356	—	—	9
	1.25	400	—	—	16
Palladium	1.30	400	—	—	25
	1.27	250	—	106.7	6
	0.93	250	—	107.88	6
Silver	0.93	250	—	107.88	6
	0.72	400	1.81	132.8	21
Caesium	0.92	400	—	—	24
	0.83	400	2.11	137.4	21
Barium	0.83	400	2.11	137.4	21
	2.2	380	—	181.4	25
Tantalum	3.7	5120	—	—	25
	1.01	250	—	195.2	6
Platinum	0.14	500	—	197.2	18
	1.71	900	—	—	17
Gold	1.14	330	—	—	8
	0.82	250	—	—	6
	1.35	450	4.54	184	15
	1.2-1.3	600	—	—	10
	1.45	700	—	—	8
Tungsten	0.85	250	—	—	6
	(not max.)	630	—	—	21
	1.29-1.40	600-1000	3.38	232.1	21

AMPLIFICATION BY MEANS OF SECONDARY ELECTRON EMISSION

Much work has been done during the past few years on the amplification by means of secondary electron emission of small electron currents, the amplification of which by thermionic valves is limited by the Schott effect and by resistance noise.

The various types of electron multiplier, as these devices are termed, are very numerous and may be classified into three main groups. The first group consists of electron multipliers using a single stage of amplification, the second of a dynamic type of electron multiplier in which an oscillation of the secondary electrons occurs between two surfaces of high sensitivity, and the third type of multipliers using multiple stages of secondary electron emission.

TABLE II. *The coefficients (δ) of secondary electron emission from complex surfaces*

Details of surface	δ max.	v. primary in volts	Reference
Lithium deposited in insufficient vacuum	3.4-4.2	300	21
Caesium deposited at room temperature	4.4 (not max.)	200	21
Cs ₂ O, Cs-Cs	5.7	300	24
Cs ₂ O, Cs, Ag-Cs	2.6-2.8	300-900	24
Ag-CsO-Cs	8.4	450	26
Magnesium deposited in a high vacuum and transferred in air to measuring tube	2.45	300	21
Aluminium target outgassed	2-3.0	3-400	21
" " "	2.24	500	18
" " "	1.80 (not max.)	140	6
" " "	2.55	350	19
Beryllium deposited in a high vacuum and transferred in air to measuring tube	4.4	600	20
Thin coat of beryllium on molybdenum base	2.5	500	25
Thick coat of beryllium on molybdenum base and subject to red heat treatment	1.6	600	25
Beryllium oxidized	4.1	—	25
Platinum on aluminium base, a function of the thickness of the platinum film	0.27-0.8	500	18
Gold contaminated with calcium	0.23-0.7	500	18
Barium after oxidation in dry oxygen	4.75	400	21
*Barium on tungsten ?presence of oxygen	1.34-2.5	300	22
*Barium on tungsten	1.23-1.74	300	22
*Barium on molybdenum	1.6-2.5	300	22
*Tungsten contaminated with thorium	1.25-1.55	300	22
*" " "	1.38-1.8	300	12
*Tungsten oxidized	1.06	300	22

* $\log_{10} \delta$ is roughly proportional to the change in work function due to contamination.

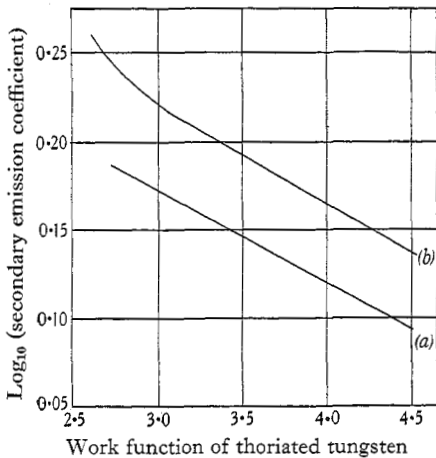


Fig. 1. The relation between the coefficient of secondary electron emission and the work function for thoriated tungsten. Curve (a) Treloar, (b) Sixtus

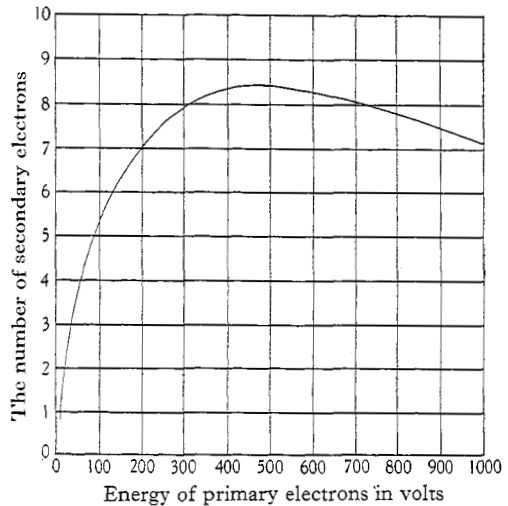


Fig. 2. The number of secondary electrons liberated from an Ag-CsO-Cs surface by each primary electron as a function of its energy

ELECTRON MULTIPLIERS USING A SINGLE STAGE OF AMPLIFICATION

The two types of electron multipliers in this group are (a) a high vacuum photocell and (b) a thermionic triode.

(a) *Secondary emission photocell.** This cell consists of an evacuated glass envelope containing an anode and two cathodes. The primary cathode is a silver deposit on one half of

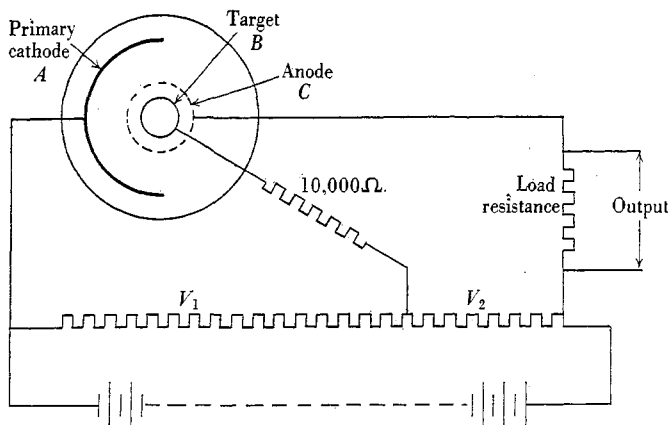


Fig. 3. Electrode arrangement and circuit of secondary emission photocell

the glass envelope and the secondary cathode or target is a silver tube supported in the centre of the envelope. The anode or collector electrode consists of a molybdenum spiral co-axial with and surrounding the secondary cathode. Both cathodes are suitably activated and are of the caesium-silver-oxide type. Fig. 3 shows the disposition of the electrodes and also a suitable circuit.

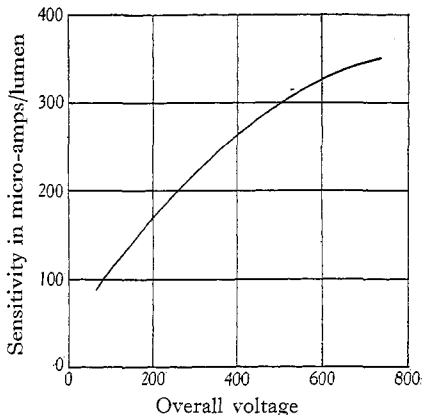


Fig. 4. The relation between sensitivity in microamperes/lumen and overall voltage of a secondary electron emission photocell

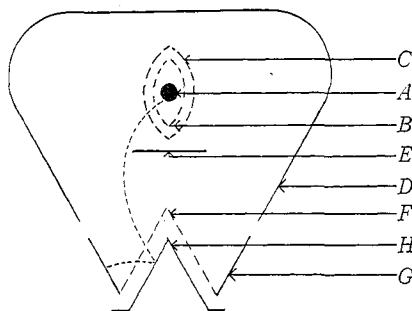


Fig. 5. Plan of triode valve with internal stage of amplification by secondary electron emission

The mode of operation is as follows: The photo-electrons emitted by the primary cathode A impinge on the secondary cathode or target B under the influence of the potential V_1 . The impact of these primary photo-electrons liberates secondary electrons from the target

* Acknowledgements are due to the General Electric Co., Ltd. for details of this type of cell.

B, and as each primary electron liberates several secondary electrons a magnification of the primary current takes place. The secondary electrons are finally collected by the anode *C* under the influence of the potential V_2 .

The advantage of this type of photocell is that in spite of its high sensitivity the background noise is extremely low compared with a gas-filled photocell under high gas amplification and is equal to that normally associated with a good high vacuum cell. A typical characteristic showing the relation between the sensitivity expressed in microamperes per lumen and the overall voltage is shown in Fig. 4.

(b) *A thermionic valve with a single stage of secondary amplification.** The plan of a thermionic valve using an internal stage of amplification by means of secondary electron emission is shown in Fig. 5.

This valve has a normal hot cathode *A*, and control grid *B*, but surrounding the latter and co-axial with it is an accelerating or screen grid *C*. A further open mesh grid *F*, secondary electron emitting cathode *H*, and anode *G*, together with the earthed screens *D* and *E*, complete the electrode structure. A suitable circuit diagram is given in Fig. 6.

The mode of operation is as follows: The hot cathode *A* and control grid *B* function in the normal manner, the potential of *B* controlling the electron emission from *A*. The electrostatic field formed by the potentials on the anode *G*, and screen grid *C*, with respect to the earthed screens *D* and *E*, is such that electrons emerging from the screen grid *C* are so bent as to travel in the direction of the grid *F*. Passing through this grid, which has an open mesh, the electrons strike the auxiliary cathode *H*, and liberate secondary electrons. These secondary electrons are then drawn out by the electrostatic field between the auxiliary cathode and the grid *F* and are collected both by it and by the anode. Thus the electron stream from *A* is modulated by the control grid *B* in the normal way, and this modulated current is amplified by the ratio of the number of secondary electrons per primary electron leaving the auxiliary cathode.

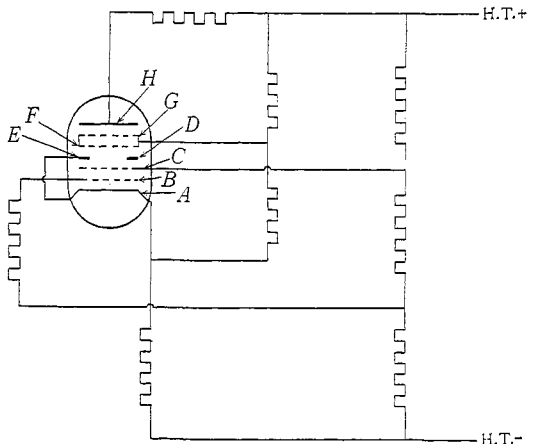


Fig. 6. Circuit diagram for use with secondary electron emission valve

A characteristic curve of a valve of this type is shown in Fig. 7. The operating point is quite critical in view of the steep slope.

DYNAMIC ELECTRON MULTIPLIERS

This type of electron multiplier, in which the secondary electrons oscillate between two sensitive surfaces, has been developed principally by Farnsworth(4). The simplest form is shown diagrammatically in Fig. 8.

The two plane electrodes *A* and *B* in an evacuated glass envelope have their surfaces sensitized for maximum secondary electron emission. A high-frequency alternating potential is applied to these electrodes and during the half-cycle of potential when *B* is positive with respect to *A* electrons liberated at the centre of *A* are accelerated across the tube towards *B* on which they impinge and liberate secondary electrons. During the next half-cycle when *A*

* Acknowledgements for details of this valve are due to the Mullard Wireless Service Co., Ltd.

becomes positive with respect to *B*, these secondary electrons are attracted towards *A* where they liberate further secondary electrons. After a predetermined number of cycles the oscillations are interrupted and the amplified secondary electron current is collected as it

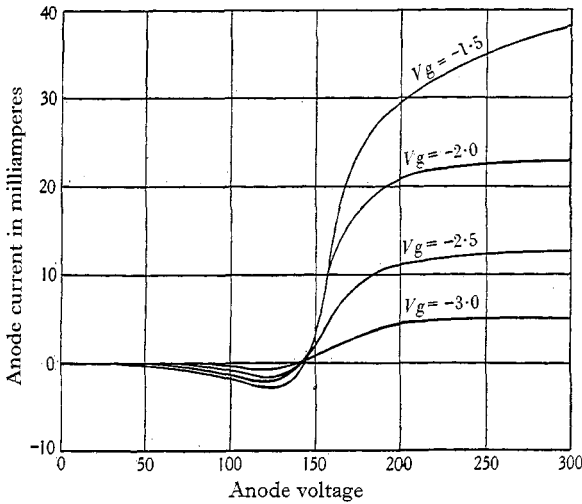
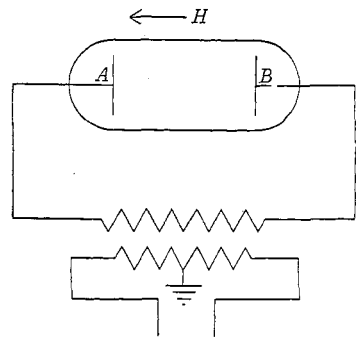


Fig. 7. Characteristic curves of secondary electron-emission valve. (V_g = control grid voltage)



To quenched oscillator
Fig. 8. A circuit for use with dynamic electron multiplier

passes into an external circuit. A form of quenched oscillator is used which interrupts itself cyclically. The gain or multiplication then depends on the frequency of the alternating potential and the time during which it is applied.

A further modification, also due to Farnsworth, is shown in Fig. 9.

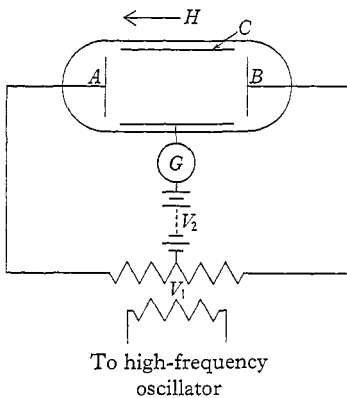


Fig. 9. An improved dynamic electron multiplier

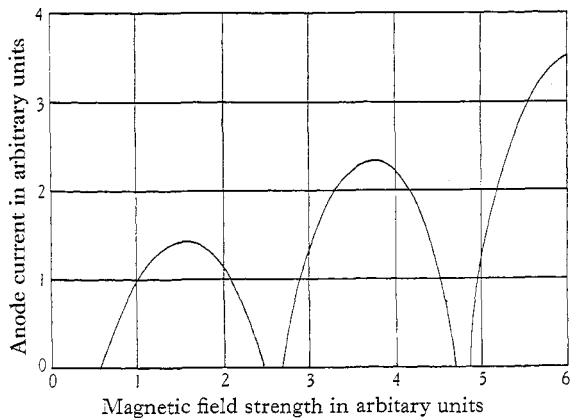


Fig. 10. A characteristic curve of improved dynamic electron multiplier

The electrode assembly is similar to that shown in Fig. 8 but with the addition of a cylindrical nickel or molybdenum electrode *C*. This electrode together with the magnetic field *H*, which is at right angles to the plane of the electrodes *A* and *B*, serves to restrict the electrons into approximately parallel paths between the targets.

The mode of operation is as follows: Assume that light illuminates the target *A* and liberates a few photo-electrons. These electrons then oscillate between *A* and *B* under the action of the alternating potential V_1 , and at the same time "drift" towards the anode under the action of the constant potential V_2 . Hence, after completing a number of impacts with *A* and *B* the amplified electron current is collected by the anode. If now the magnitude of this current as measured by the meter *G* is plotted as a function of the anode voltage, a characteristic similar to that shown in Fig. 10 is obtained.

On increasing the amplitude of the radio-frequency voltage, which is normally of the order of 50 V R.M.S., the peaks become broader and eventually the curve becomes continuous. Changes in the frequency of the alternating voltage change the relative positions of the peaks. The theoretical explanation of the functioning of this multiplier is incomplete.

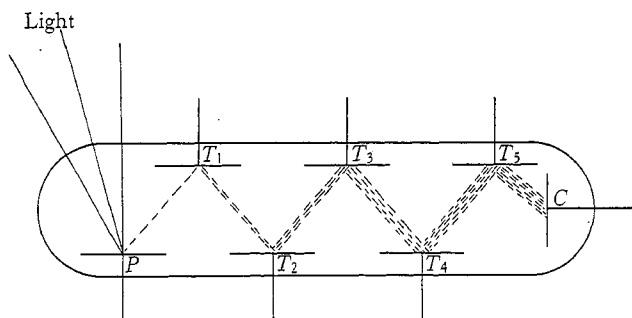


Fig. 11. A simple multiple stage electron multiplier

These two examples of electron multipliers, although simple in principle, have several disadvantages. The amplification tends to vary owing to practical difficulties in controlling accurately the frequency and amplitude of the alternating potential. The time constant of the quenched oscillator may also vary, and so change the number of impacts made, and hence the amplification. The ratio of background to signal noise is high. This type of multiplier is not now in general use.

ELECTRON MULTIPLIERS USING MULTIPLE STAGES OF AMPLIFICATION

The general feature of electron multipliers in this group is that the secondary electrons liberated at the first target by the primary electrons are accelerated towards a second target instead of returning to the photo-electric cathode. The secondary electrons liberated at this second target are then accelerated towards another target. Reference to Fig. 11 will make this process clear.

The photo-electrons, initially liberated at *P*, are accelerated by an electrostatic field towards the target T_1 , which has been sensitized for maximum secondary electron emission, on which they impinge liberating secondary electrons. These secondary electrons are then accelerated by the electrostatic field on to the target T_2 liberating further secondary electrons. This process may be repeated as often as desired within reasonable limits. Finally the secondary electrons from T_3 are collected by the plate *C*. Here the gain or amplification may be given as

$$I_s = I_p \delta^n,$$

where I_p is the initial and I_s the final electron currents, δ is the coefficient of secondary

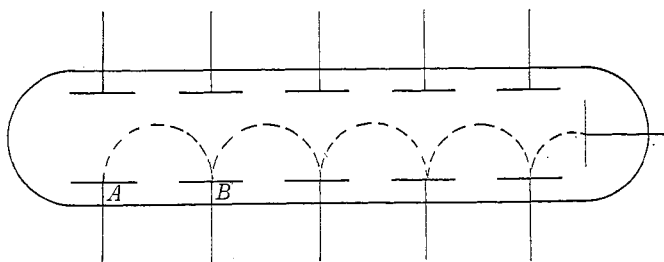


Fig. 12. The electrode assembly of an electron multiplier using crossed electrostatic and magnetic fields

electron emission and n is the number of stages. Also the overall gain is given by δ^n , so that when δ is large, 7 to 8, overall gains of the order of 10^6 to 10^8 are easily obtained with 7 to 8 stages.

The electron multiplier shown in Fig. 11 works very inefficiently, as the electrons tend to go straight along the tube to the collector plate C, without hitting any of the targets on the way. To avoid this some means of focusing the electrons on successive targets is required. The practical design of these multipliers has proceeded along two different lines: the first using crossed electrostatic and magnetic fields and the second using only electrostatic fields.

(a) *Electron multipliers using crossed electrostatic and magnetic fields.** Fig. 12 shows the internal electrode assembly of a multiplier of this type⁽²⁶⁾, and an experimental multiplier together with its electro-magnet is shown in Fig. 13.

This multiplier consists of two rows of plane electrodes, the bottom row being coated with a suitable secondary electron-emitting material. The upper row, Fig. 11, serves to maintain a transverse electrostatic field between the two sets of electrodes. A magnetic field is maintained at right angles to the electrostatic field and to the axis of the tube. The electrons liberated at A in all directions are now deflected by the combined fields and focused on to the target B .

The initial energy of the secondary electrons causes them to depart from their true cycloidal path, and so causes a certain amount of defocusing. The average energy of these secondary electrons from an

Ag-CsO-Cs surface is only of the order of 3 eV and hence the spread of the beam does not become serious except with large numbers of stages. The effect would be to reduce the stage gain of the later stages of the multiplier owing to some of the electrons missing their target and falling into the fields of adjacent electrodes. However, multipliers having twelve stages have been built without any noticeable falling off in the gain per stage.

* Acknowledgements are due to Messrs A. C. Cossor, Ltd. for the loan of an electron multiplier of this type with which the following data were obtained.

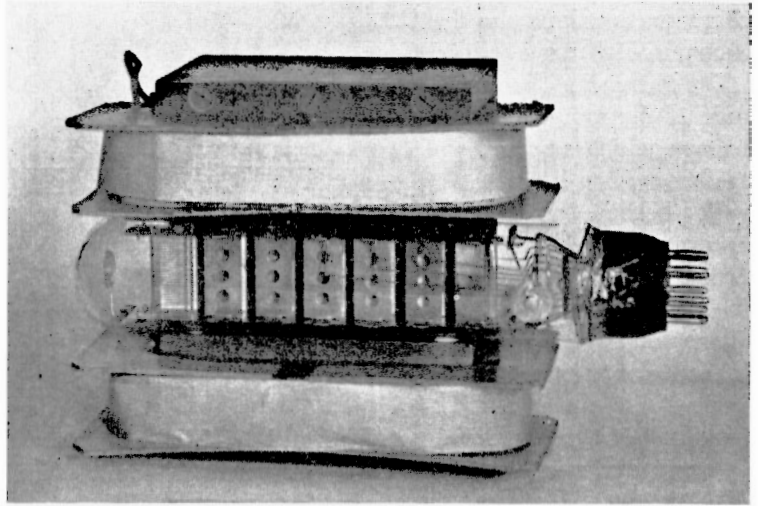


Fig. 13. An experimental electron multiplier with electro-magnet

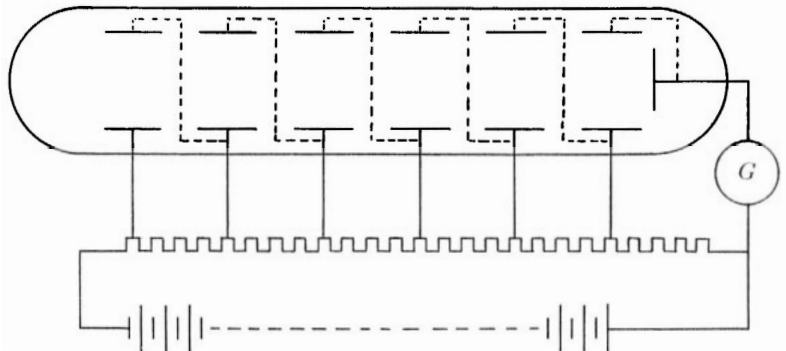


Fig. 14. Circuit for use with experimental multiplier shown in Fig. 13.
The internal connexions are shown dotted

Fig. 14 shows a circuit diagram of the complete multiplier equipment which has proved very satisfactory. Fig. 15 shows the effect on the gain of a six-stage multiplier of varying the magnetic field while using an electrostatic field of fixed magnitude. Fig. 16 shows the dependence of the gain of a six-stage multiplier on the magnitude of the electrostatic field with a fixed magnetic field. Fig. 17 shows the relation between the gain of a six-stage multiplier and the overall voltage with a fixed magnetic field strength.

The curves in Figs. 15 and 16 show secondary peaks as well as the main primary one. These are due to electrons following more complicated paths either being reflected by the upper electrostatic field plates or by striking every alternate target.

(b) *Electron multipliers using electrostatic fields.* Electron multipliers using only electrostatic fields consist of two types, the first using solid targets and the second grid-mesh targets.

(i) *Electrostatic multipliers using solid targets.* The principal multipliers of this type depend for their successful operation on the production of electrostatic lens systems similar to those found in cathode-ray oscillograph tubes and electron microscopes. The function of this lens will be made clearer by reference to Fig. 18.

Two cylinders *A* and *B*, each closed at one end, are separated by a small distance and a potential difference is applied between them. Electrons of low initial energy are liberated in all directions at the point *X*. These are attracted by the positively charged cylinder *B* and are brought to focus at *Y* by the lens action of the electrostatic fields.

Two practical multipliers are shown in Fig. 19 and are known as *L* and *T* types from the nature of their shapes.

Multipliers of this type suffer from the disadvantage of using relatively high voltages (200–400 V per stage) which introduces constructional difficulties when a number of stages is used. Space-charge effects may also be set up when currents of the order of milliamperes are drawn from the targets, owing to the low value of the electrostatic field at the point of collection.

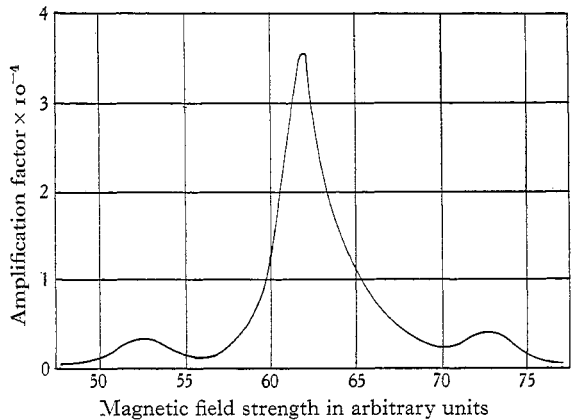


Fig. 15. The variation of the amplification factor of a six-stage electron multiplier as a function of the magnetic field strength

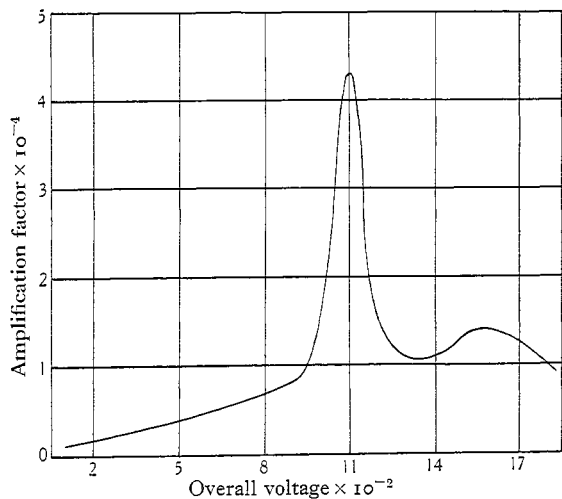


Fig. 16. The variation of the amplification factor of a six-stage electron multiplier as a function of the electrostatic field strength

Another type of multiplier which can be included in this group has been developed by Farnsworth (Fig. 20).

The glass tube has on its walls a nickel deposit of such a thickness that the resistance between the connexions *A* and *B* is of the order of 2 MΩ. This nickel surface is then coated

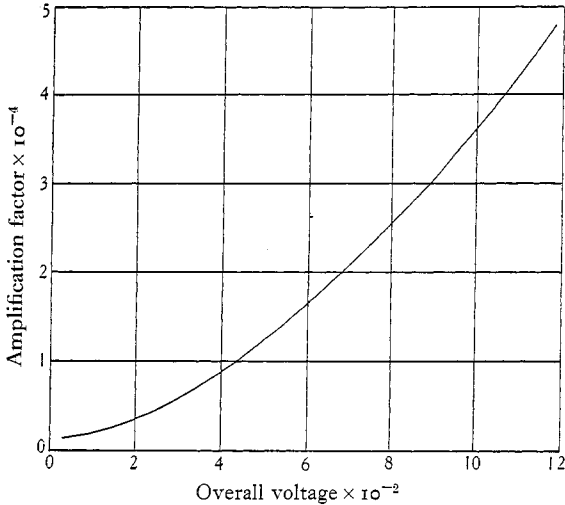


Fig. 17. The variation of the amplification factor as a function of the overall voltage using the optimum magnetic field strength

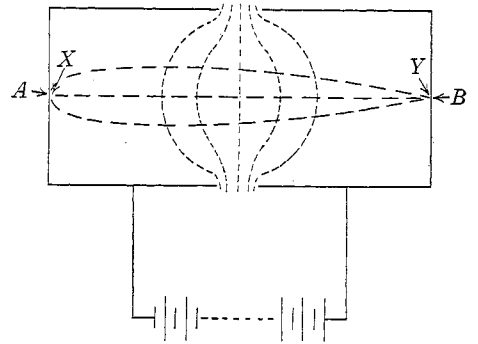


Fig. 18. An electrostatic lens system

with a suitable secondary electron-emitting material, the whole being so processed that the final resistance between *A* and *B* is greater than 1 MΩ. The centre electrode consists of a fine wire strung along the axis of the tube and terminated in a flat circular plate *P*.

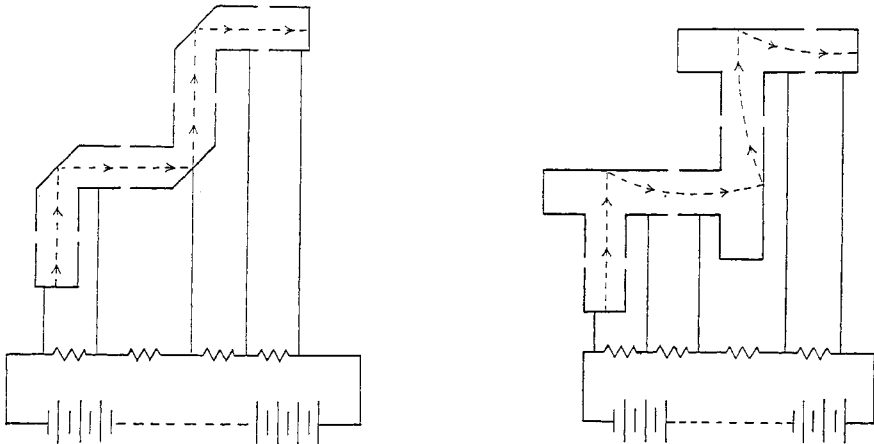


Fig. 19. *L* and *T* types of electron multipliers

Photo-electrons liberated at *X* are attracted to the central electrode by reason of its positive potential and at the same time they are attracted along the axis of the tube by reason of its increasing positive potential. The resultant path is approximately as shown dotted in Fig. 19. Only a small percentage of the electrons strike the central electrode by reason of its

small diameter and the direction of their acceleration, and hence they mostly impinge upon the opposite wall of the tube. Here they liberate secondary electrons which are in turn accelerated both across and down the tube. The number of impacts made and hence the gain is governed by the overall dimensions of the tube and the total applied voltage. The final electron current is collected by the plate *P*.

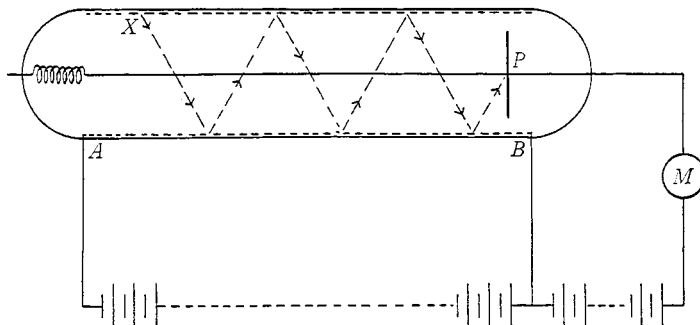


Fig. 20. An electron multiplier with a high resistance secondary electron-emitting surface and self-adjusting potential distribution

It is reported that this last type of multiplier is satisfactory only where amplifications of the order of a few hundred times are required. The problems of heat dissipation inside the tube and of voltage distribution along the nickel resistance deposit become increasingly difficult when attempts are made to obtain higher gains.

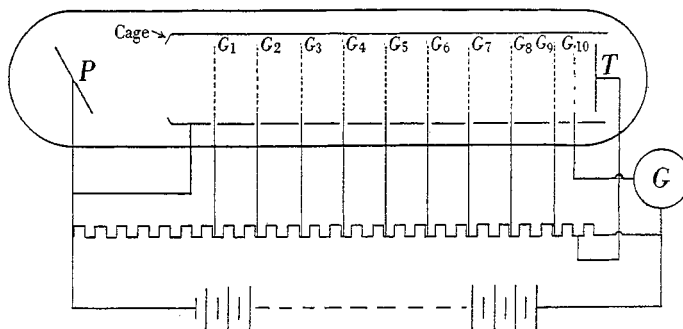


Fig. 21. The electrode structure of a grid-mesh type electron multiplier

(ii) Electrostatic multipliers using close-mesh targets.* The general principle underlying this type of multiplier is that the low energy secondary electrons liberated on one side of a secondary electron-emitting wire grid can be drawn through the meshes by a positive electrostatic field placed on the opposite side to the incident beam of electrons, and subsequently accelerated on to an adjacent grid.

The electrode system of one type of multiplier in this class is shown in Fig. 21. An experimental model, with part of the focusing cylinder cut away to show the multiplying grids, is shown in Fig. 22.

It consists of a photo-electric cathode *P* and a number of sensitized grids G_1 – G_9 arranged inside but insulated from a metal cylinder or cage. The method of operation is as follows:

* Acknowledgements for certain information and the loan of a multiplier of the type shown in Figs. 21 and 22 are due to Messrs Baird Television, Ltd.

Electrons liberated at P are attracted by the positive potential on the first grid G_1 , on which they impinge, liberating secondary electrons. These secondary electrons are accelerated to G_2 where they liberate further electrons. This is repeated to G_9 . Here the electrons are accelerated to T through the open-mesh non-sensitized grid G_{10} , where a final multiplication

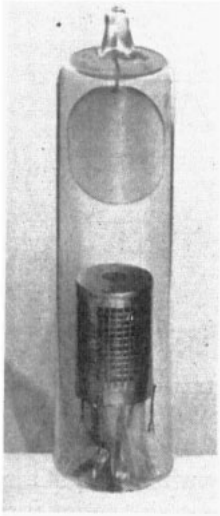


Fig. 22. An experimental grid-mesh electron multiplier

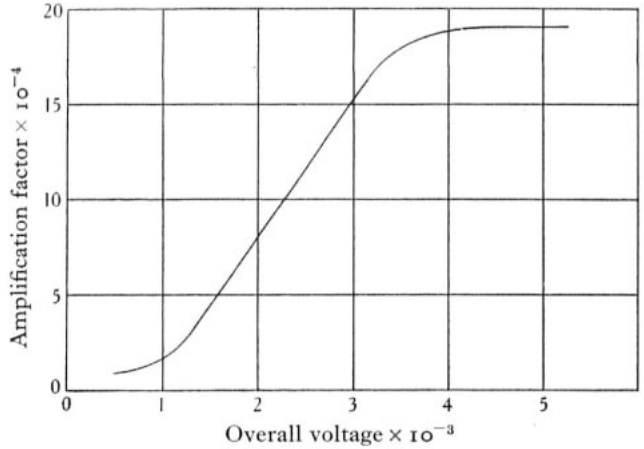


Fig. 23. The relation between the overall voltage and the gain of a nine-stage grid-mesh multiplier

of 8–9 is obtained due to impact on a solid target. The secondary electrons liberated from the plate T are collected by the positively charged open-mesh grid, G_{10} .

The cage, which is at a negative potential with respect to grids G_1 – G_{10} , prevents the electrons spreading by reason of their mutual repulsion. This spreading of the electron beam

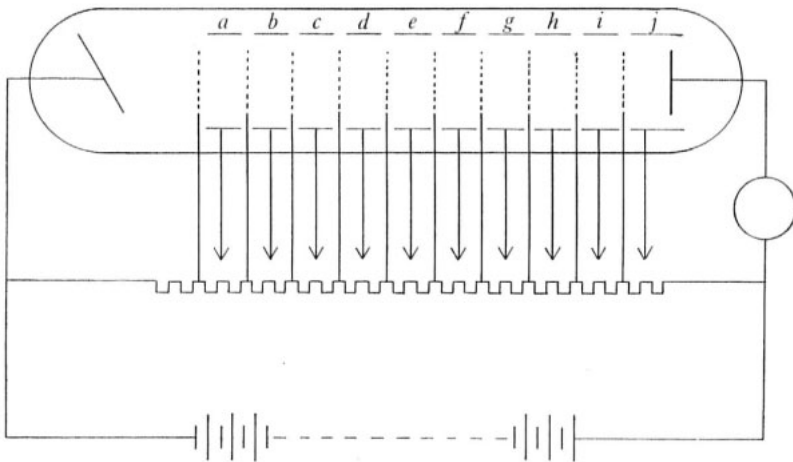


Fig. 24. A modified grid-mesh multiplier with independent focusing for each stage

would result in a loss of efficiency or amplification, due to electrons missing the sensitized grids.

Fig. 23 shows the relationship between the gain and the overall potential of a multiplier of this type using nine grids.

The maximum current which can be permitted to flow in the output circuit is governed by the temperature rise of the multiplying grids. If this is allowed to rise to too high a value the secondary electron-emitting surfaces will be destroyed. With the type shown in Figs. 21 and 22 this peak current is approximately 1 ma.

It can be shown, by coating the multiplying grids with fluorescent materials, that this current is focused on to an area of less than 1 sq. mm. This is due to the relatively very strong electrostatic field between the final multiplying grid and the focusing cylinder. Reference to the circuit given in Fig. 21 shows that this field is produced by a voltage approximately equal to the overall voltage of the multiplier. The effect of this acute focusing is that the grid is locally heated to a temperature much above that of the remainder. Hence, if the electron current could be spread over the whole of the multiplying grid the maximum permissible current could be much greater.

The further modification, shown in Fig. 24, overcomes this difficulty by arranging for the focusing of each stage to be under separate control.

Here the metal focusing cylinder, Fig. 21, is replaced by a number of metal rings *a, b, c*, with multiplying grids interposed. Each grid and focusing ring is brought out to a separate terminal so that their relative potentials, and hence the spread of the electron beam, can be separately controlled. The final current can thus be spread uniformly over the whole of the multiplying grid and therefore the maximum permissible current can be greatly increased.

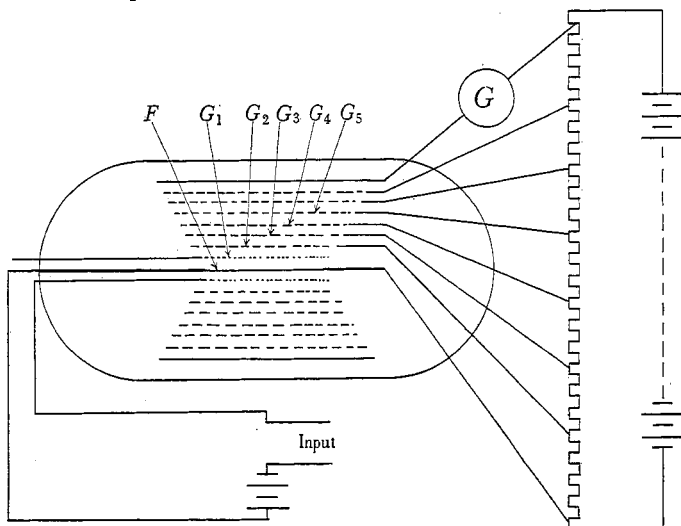


Fig. 25. A "Multipactor" electron multiplier using sensitized co-axial grid-mesh cylinders

The general characteristics of this type of multiplier are very similar to those given for the preceding type. Another type of grid-mesh multiplier, which is known as a "Multipactor", consists of a number of co-axial grid-mesh cylinders as shown diagrammatically in Fig. 25.

There are, as in all these types of multipliers, many slight modifications, but the example shown above is representative of the type. The primary source of electrons is a hot filament, *F*, which may of course be replaced by a photoelectric cathode. This filament is surrounded by an unsensitized grid which is, in turn, surrounded by a secondary electron-emitting grid. Further multiplying grids can be added if desired. The filament *F*, unsensitized grid *G*₁, and first multiplying grid *G*₂, function in the same manner as the filament, control grid and anode of the conventional triode valve, the grid controlling the electron current flowing from the filament to the anode.

The primary electrons on reaching the first anode or second grid, *G*₂, Fig. 25, liberate low energy secondary electrons. These secondary electrons are then drawn through the grid meshes and are accelerated by the potential *V*₂, on to the grid, *G*₃. Here further amplification by secondary electron emission takes place. The final electron current is collected by the anode.

The result of this "internal" amplification is to increase the mutual conductance of the initial filament, grid and anode assembly in the following manner:

$$g_{mf} = g_{mi} \delta^n,$$

where g_{mf} and g_{mi} are the final and initial mutual conductances, δ is the coefficient of secondary electron emission and n is the number of stages of amplification.

REFERENCES

- (1) Slepian Patent No. 1,450,265, April 1923.
- (2) JARVIS and BLAIR. Patent No. 1,903,569, April 1933.
- (3) IAMS and SALZBERG. *Proc. Inst. Radio Eng.* **23**, p. 55 (1935).
- (4) FARNSWORTH. *J. Franklin Inst.* **218**, p. 411 (Oct. 1934).
- (5) — *Electronics*, **7**, p. 242 (1934).
- (6) — *Phys. Rev.* **25**, p. 43 (Jan. 1925).
- (7) — *Phys. Rev.* **27**, p. 413 (Apr. 1926).
- (8) PETRY. *Phys. Rev.* **28**, p. 362 (Aug. 1926).
- (9) — *Phys. Rev.* **26**, p. 346 (Sept. 1925).
- (10) KREFFT. *Phys. Rev.* **31**, p. 202 (Feb. 1928).
- (11) HYATT and SMITH. *Phys. Rev.* **32**, p. 929 (Dec. 1928).
- (12) SIXTUS. *Ann. der Phys.* **3**, p. 1017 (1929).
- (13) FARNSWORTH. *Phys. Rev.* **34**, p. 679 (Sept. 1, 1929).
- (14) RAO. *Proc. Roy. Soc. A*, **128**, p. 41 (July 1930).
- (15) AHEAM. *Phys. Rev.* **38**, p. 1858 (Nov. 15, 1931).
- (16) COPELAND. *J. Franklin Inst.* **215**, p. 593 (May 1933).
- (17) TURNBULL and COPELAND. *Phys. Rev.* **45**, p. 763 (May 15, 1934).
- (18) COPELAND. *Phys. Rev.* **48**, p. 96 (July 1, 1935).
- (19) WARNECKE. *J. de Physique et le Radium*, **7**, p. 270 (June 1936).
- (20) KURRELMAYER and HAYNER. *Phys. Rev.* **52**, p. 952 (Nov. 1, 1937).
- (21) BRUNING and DE BOER. *Physica*, **4**, p. 473 (June 1937).
- (22) TRELOAR. *Proc. Phys. Soc.* **49**, p. 392 (July 1937).
- (23) FRÖHLICH. *Ann. der Phys.* **13**, No. L, p. 229 (1932).
- (24) KHEBRIKOV and KORSHUNOVA. *Tech. Phys. U.S.S.R.* **5**, No. 5, p. 363 (1938).
- (25) SCHNEIDER. *Phys. Rev.* **54**, p. 185 (Aug. 1, 1938).
- (26) ZWORYKIN, MORTON and MALTER. *Proc. Inst. Radio Eng.* **24**, p. 351 (1936).

ON METHODS OF SYNCHRONIZING THE ILLUMINATION FOR AN ULTRACENTRIFUGE. BY YNGVE BJÖRNSTÅHL, PH.D., Laboratory of Physical Chemistry, Upsala University, Sweden

[MS. received 20th February 1939]

ABSTRACT. The ultracentrifuge makes it possible to measure the sedimentation velocity by means of optical methods while the centrifuge is running at very high speeds. If centrifuge rotors of oval shape are used in order to increase the bursting strength, an intermittent light source is necessary. The light flashes must be in synchronism with the speed of the rotor. Several methods of synchronizing the illumination are described.

In order to determine the weight of heavy molecules two different methods have been devised by Svedberg⁽¹⁾. The solution to be investigated is poured into a cell fixed in the rotor of a centrifuge. The concentration in different layers of the liquid is determined by optical methods while the centrifuge is running. The molecular weight can be calculated either from the sedimentation velocity in strong centrifugal fields or from the sedimentation equilibrium attained by prolonged centrifuging.

Svedberg has made an attempt to use rotors of oval shape in order to increase the